

UC Merced

UC Merced Previously Published Works

Title

Cooperative KaiA-KaiB-KaiC interactions affect KaiB/SasA competition in the circadian clock of cyanobacteria.

Permalink

<https://escholarship.org/uc/item/4s0388g5>

Journal

Journal of Molecular Biology, 426(2)

Authors

Tseng, Roger
Chang, Yong-Gang
Bravo, Ian
et al.

Publication Date

2014-01-23

DOI

10.1016/j.jmb.2013.09.040

Peer reviewed



Published in final edited form as:

J Mol Biol. 2014 January 23; 426(2): 389–402. doi:10.1016/j.jmb.2013.09.040.

Cooperative KaiA–KaiB–KaiC Interactions Affect KaiB/SasA Competition in the Circadian Clock of Cyanobacteria

Roger Tseng^{1,2}, Yong-Gang Chang¹, Ian Bravo¹, Robert Latham¹, Abdullah Chaudhary³, Nai-Wei Kuo¹, and Andy LiWang^{1,2,4,5}

¹-School of Natural Sciences, University of California, Merced, CA 95343, USA

²-Quantitative and Systems Biology Graduate Group, University of California, Merced, CA 95343, USA

³-School of Engineering, University of California, Merced, CA 95343, USA

⁴-Chemistry and Chemical Biology, University of California, Merced, CA 95343, USA

⁵-Center for Chronobiology, Division of Biological Sciences, University of California, San Diego, La Jolla, CA 92093, USA

Abstract

The circadian oscillator of cyanobacteria is composed of only three proteins, KaiA, KaiB, and KaiC. Together, they generate an autonomous ~24-h biochemical rhythm of phosphorylation of KaiC. KaiA stimulates KaiC phosphorylation by binding to the so-called A-loops of KaiC, whereas KaiB sequesters KaiA in a KaiABC complex far away from the A-loops, thereby inducing KaiC dephosphorylation. The switch from KaiC phosphorylation to dephosphorylation is initiated by the formation of the KaiB–KaiC complex, which occurs upon phosphorylation of the S431 residues of KaiC. We show here that formation of the KaiB–KaiC complex is promoted by KaiA, suggesting cooperativity in the initiation of the dephosphorylation complex. In the KaiA–KaiB interaction, one monomeric subunit of KaiB likely binds to one face of a KaiA dimer, leaving the other face unoccupied. We also show that the A-loops of KaiC exist in a dynamic equilibrium between KaiA-accessible exposed and KaiA-inaccessible buried positions. Phosphorylation at the S431 residues of KaiC shift the A-loops toward the buried position, thereby weakening the KaiA–KaiC interaction, which is expected to be an additional mechanism promoting formation of the KaiABC complex. We also show that KaiB and the clock-output protein SasA compete for overlapping binding sites, which include the B-loops on the CI ring of KaiC. KaiA strongly shifts the competition in KaiB's favor. Thus, in addition to stimulating KaiC phosphorylation, it is likely that KaiA plays roles in switching KaiC from phosphorylation to dephosphorylation, as well as regulating clock output.

Correspondence to Andy LiWang: 5200 North Lake Road, Merced, CA 95340, USA. Telephone: (209) 777-6341. aliwang@ucmerced.edu.

Appendix A. Supplementary data

Supplementary data to this article can be found online at <http://dx.doi.org/10.1016/j.jmb.2013.09.040>.

Keywords

cooperativity; phosphorylation; NMR; protein; fluorescence

Introduction

Evolution of life under daily swings of ambient light and temperature produced timekeeping systems called circadian clocks [1]. These cellular clocks prepare organisms for environmental oscillations by imposing circadian rhythms on gene expression, metabolism, physiology, and behavior in-phase with the rising and setting of the sun. These internal rhythms originate from the oscillator components of circadian clocks and are transmitted downstream through output pathways, resulting in clock control over cellular processes with important consequences to health and reproductive fitness [2–7]. At the other end, environmental cues entrain the oscillators through sensory input pathways. However, the mechanisms of biological timekeeping at the molecular level remain largely unresolved.

With regard to elucidating the molecular mechanics of circadian oscillators, most of the inroads have been made in the cyanobacterial system, which is composed of only three proteins, KaiA, KaiB, and KaiC [8] (Fig. 1). A mixture of these proteins from *Synechococcus elongatus* with ATP produces an autonomous, entrainable, and temperature-compensated circadian rhythm of KaiC autophosphorylation and autodephosphorylation [9–11]. Recently, circadian rhythms of KaiC phosphorylation were also reconstituted *in vitro* using *Thermosynechococcus elongatus* proteins [12]. KaiC is a homohexamer in which each subunit is composed of two RecA-like domains, called CI and CII [13,14]. The CI and CII domains self-associate into rings and stack together similar to two donuts [15,16]. KaiA stimulates phosphorylation [17] by binding to the so-called A-loops of KaiC [18–20]. The A-loops are located at the pore of the CII ring. Each CII domain contains two residues, S431 and T432, which in the presence of KaiA phosphorylate ($S \rightarrow pS$ and $T \rightarrow pT$) in the following order: $ST \rightarrow SpT \rightarrow pSpT$ [21,22]. Upon phosphorylation of S431, the CII ring transitions from loose to tight and then stacks on the CI ring [23]. This stacking interaction exposes part of the KaiB binding site on CI [24]. KaiB binds to KaiC and inactivates KaiA [21,22]. KaiC then passes sequentially through the phosphoforms $pSpT \rightarrow pST \rightarrow ST$, whereupon the rings unstack and a new cycle begins. This ring-ring communication explained how phosphorylation on the CII ring could induce new protein-protein interactions on the CI ring. Recently, it was demonstrated that dephosphorylation likely proceeds through phosphoryl transfer from KaiC to bound ADP molecules, followed by hydrolysis of the newly formed ATP intermediates [25,26].

With regard to entrainment, instead of having photoreceptor-mediated input pathways, the cyanobacterial clock relies on metabolic products of photosynthesis [27,28]. Oxidized quinones signal the onset of darkness by directly binding to and inactivating KaiA [29,30] and the input pathway protein CikA [31–34], whereas high ADP/ATP ratios, which act directly on KaiC, are a measure of the duration of darkness [35]. Through output pathways, the cyanobacterial clock controls cellular processes such as genome-wide gene expression [36–39] and cell division [40,41]. The output pathway protein SasA [42], a sensor histidine

kinase, receives timing signals from the oscillator through direct interactions of its N-terminal domain with KaiC. This interaction stimulates SasA phosphorylation [43] and subsequent phosphoryl transfer to and activation of the transcription factor RpaA [44]. Whereas SasA can bind to each phosphoform of KaiC [45], KaiB only binds to KaiC when the S431 residues are phosphorylated [21,22], and it can displace SasA from those phosphoforms [12,46]. Interestingly, stimulation of CikA by the KaiB–KaiC complex during the subjective night induces dephosphorylation of RpaA [47]. Thus, rhythms in KaiB–KaiC binding may regulate clock output by controlling sequential and reciprocal action of SasA and CikA on RpaA. Recently, we showed that both SasA [23] and KaiB [24] bind to the CI domain of KaiC, suggesting that they compete for overlapping binding sites.

Until now, it has been thought that KaiA only stimulates KaiC phosphorylation [17,48] and signals the onset of darkness [27]. In other words, KaiA has not been presumed to play active roles in the dephosphorylation of KaiC or clock output. Here, using proteins from *T. elongatus*, we investigated whether those two presumptions are warranted. We show that, in fact, KaiA plays a cooperative role in the assembly of the KaiA–KaiB–KaiC dephosphorylation complex and that decreasing KaiA–KaiC affinities during KaiC phosphorylation enhances this cooperativity. We also show that KaiA promotes the displacement of SasA by KaiB from KaiC, implicating KaiA as one of the regulators of clock output. Apparently, a dimer of KaiA binds only one KaiB monomer. Additionally, we show that KaiB and SasA bind to the B-loop of the CI domain of KaiC.

Results

Resolving whether the N-terminal domains of KaiA are necessary for binding KaiB

The N-terminal domains of KaiA from *S. elongatus* have recently been demonstrated to play a critical role in entrainment by sensing oxidized quinones [27]. An X-ray crystal structure of KaiA verified that the N-terminal domains bind directly to the oxidized form of quinone analog 2,5-dibromo-3-methyl-6-isopropyl-p-benzoquinone [30]. Less clear is the role of the N-terminal domains in generating KaiC phosphorylation rhythms. Recent electron microscopy (EM) studies have suggested that, in order for KaiC to dephosphorylate, KaiB sequesters monomeric subunits of KaiA by binding exclusively to its N-terminal domains [46]. If correct, the N-terminal domains of KaiA would be necessary for the generation of phosphorylation rhythms. However, electron spin resonance spectroscopy suggests that the C-terminal domains of KaiA bind KaiB [49]. Additionally, *Anabaena* sp. strain PCC-7120, which supposedly displays circadian rhythms [50], lacks N-terminal domains [51]. Also, truncating the N-terminal domains of KaiA did not abolish *in vivo* rhythms of bioluminescence [52]. We therefore wanted to clarify these contradicting models. In Fig. 1, we provided a list of the different constructs of KaiA, KaiB, and KaiC used in this study.

Here, using size-exclusion chromatography of *T. elongatus* proteins, we found that a KaiA construct, ^NKaiA, which lacked its N-terminal domains by truncating before residue S147 (Fig. 1a), formed a stable ternary complex with KaiB* (a dimeric variant of KaiB) [24] and CI* (a monomeric variant of the CI domain) [24] (Fig. 2a, left panel). Because KaiB* binds to CI as a monomer [24], it is likely that KaiB* is a monomer in this ternary complex as well. Next, we tested formation of ^NKaiA–KaiB*–CI* by NMR. Chemical shift perturbations in

methyl-TROSY (transverse relaxation optimized spectroscopy) NMR [53] spectra of U- ^{15}N , ^2H]-Ile δ 1- ^{13}C , ^1H] $^{\text{N}}$ KaiA in the presence of unlabeled KaiB* and CI* (Fig. 3a, columns 1 and 2) also indicated complex formation, corroborating our chromatography results. Identical spectra were obtained when using KaiB (wild type) instead of KaiB* to form the $^{\text{N}}$ KaiA–KaiB–CI* complex (Fig. 3a, column 3), suggesting that these interactions are not artifacts from using a mutant of KaiB. As further evidence that the N-terminal domains of KaiA are not necessary for KaiA–KaiB interactions, a full phosphorylation cycle was observed using $^{\text{N}}$ KaiA instead of KaiA (Fig. S3a and b). Thus, the recent model in which the N-terminal domains of KaiA are necessary for KaiA–KaiB binding [46], albeit in the *S. elongatus* system, may need to be revised. Previously, we showed that a construct of KaiA missing residues 1–179 could not be sequestered by KaiB [18], which together with the data here suggests that the linker connecting the N- and C-terminal domains, residues 147–179, plays a role in KaiA–KaiB interactions. $^{\text{N}}$ KaiA was used for NMR experiments because of its smaller size and labeled for fluorescence experiments because it retains only one of four naturally occurring cysteinyl residues (C272) for convenient labeling with thiol-reactive fluorophores.

Assembly of the KaiA–KaiB–KaiC complex is a cooperative process

Even after several hours of incubation, there were no detectable interactions between $^{\text{N}}$ KaiA and KaiB (Fig. 3a, column 4). However, CI* significantly enhanced $^{\text{N}}$ KaiA–KaiB binding (Fig. 3a, column 3). Similarly, others have observed that KaiC enhances the otherwise weak interaction between KaiA and KaiB [11,13,54]. In contrast to KaiB, KaiB* bound to $^{\text{N}}$ KaiA even in the absence of CI* (Fig. 2a, left panel; Fig. 3a, columns 5 and 6). Recall that the stable forms of free KaiB and KaiB* are homotetramer [55–57] and homodimer [24], respectively. Based on our findings, we propose that the dimer is closer to the conformation that binds KaiC and KaiA than the tetramer. This idea is supported by recent findings that KaiB* binds more rapidly to CI* than does KaiB [12,24].

As with KaiB, the weak $^{\text{N}}$ KaiA–KaiB* interaction was significantly enhanced by CI*. Free $^{\text{N}}$ KaiA or KaiB* was undetectable by gel-filtration chromatography in the presence of CI*, in contrast to when CI* was absent (Fig. 2a, left panel). Similarly, NMR spectra of labeled $^{\text{N}}$ KaiA showed complete KaiB* binding in the presence of CI* (Fig. 3a, column 2) but incomplete binding without CI* (Fig. 3a, columns 5 and 6). The absence of an observable interaction between just $^{\text{N}}$ KaiA and CI* (Fig. 3a, column 7; Fig. S1a) suggests that CI* facilitates KaiA–KaiB binding solely through interactions with KaiB. The observation that the majority of the NMR peaks of KaiB*-bound $^{\text{N}}$ KaiA had the same chemical shifts in the presence and absence of CI* also supports this notion (Fig. 3a, columns 2 and 3 and columns 5 and 6). Although $^{\text{N}}$ KaiA did not interact with CI*, NMR spectra showed, as expected, that $^{\text{N}}$ KaiA interacted with CII*, a monomeric variant of the CII domain [18] (Fig. 3a, column 8). These observations support the model in which KaiA has two distinct binding sites, the A-loop during KaiC phosphorylation [18] and KaiB during dephosphorylation [24,54,58].

Now that we have demonstrated that CI* facilitates KaiA–KaiB binding, we tested the extent to which KaiA facilitates KaiB–KaiC binding. We measured the apparent dissociation

constants, K_D^{app} , for the KaiB–CI* complex in the presence and absence of saturating amounts of KaiA (wild type), by monitoring the fluorescence anisotropy of labeled KaiB (Fig. 3b). Indeed, we found that KaiA decreased the K_D^{app} 10-fold, from $20.5 \pm 1 \mu\text{M}$ to $2.0 \pm 0.4 \mu\text{M}$, indicating positive cooperativity (cooperativity factor of 0.10 ± 0.02). Thus, our results suggest that the switch from KaiC phosphorylation to dephosphorylation is promoted by cooperative formation of the KaiA–KaiB–KaiC complex.

Estimating the stoichiometry of the KaiA–KaiB complex

So far, the structural details of the KaiA–KaiB complex in the dephosphorylation phase of KaiC remain largely unclear. The stoichiometry of the KaiA–KaiB complex was recently estimated by gel-filtration chromatography to be a dimer of KaiB bound to a dimer of KaiA [49]. In a two-fold symmetric complex, each symmetry-related pair of spins would produce a single observable NMR signal. However, the number of peaks in methyl-TROSY spectra of U- ^{15}N , ^2H -Ile δ 1- ^{13}C , ^1H $^{\text{N}}$ KaiA almost doubled upon binding KaiB*, not counting the peaks that corresponded to unbound $^{\text{N}}$ KaiA (Fig. S2). In the spectrum of free $^{\text{N}}$ KaiA, there were nine methyl peaks as was expected for a symmetric homodimer with nine isoleucine residues per subunit [59]. However, 16 new $^{\text{N}}$ KaiA peaks appeared upon adding unlabeled KaiB*. These new peaks persisted after forcing all $^{\text{N}}$ KaiA into the complex by adding CI* (Fig. 3a, column 1 and 2), indicating that the new peaks were from the bound form of $^{\text{N}}$ KaiA. This 1.8-fold increase in the number of NMR peaks suggests that the symmetry of $^{\text{N}}$ KaiA was broken by KaiB*. Although dramatic changes in the ^{15}N TROSY spectra of ^{15}N , ^2H KaiB* upon binding unlabeled $^{\text{N}}$ KaiA suggested that KaiB* changed its structure globally, the number of peaks remained similar (Fig. S5a). A model consistent with these observations is one in which KaiB binds as a monomer to one face of the $^{\text{N}}$ KaiA dimer. This binding may distort the other face such that a second KaiB monomer cannot bind.

The idea of a monomeric subunit of KaiB binding to a KaiA dimer is also supported by size-exclusion chromatography (Fig. 2a, right panel). We ran mixtures of $^{\text{N}}$ KaiA:KaiB*:CI* at monomer molar ratios of 1:1:1, 2:1:1, and 3:1:1. At 1:1:1, both KaiB*–CI and $^{\text{N}}$ KaiA–KaiB*–CI complexes were observed. However, in the 2:1:1 mixture, the KaiB*–KaiC complex disappeared and, similar at 1:1:1, no free $^{\text{N}}$ KaiA was detected. Only at the 3:1:1 ratio was free $^{\text{N}}$ KaiA observed. Together, the data suggest that one subunit of KaiB binds one subunit of CI and two subunits of KaiA at the C-terminal and linker regions. The hydrophobic nature of the dimer interface of KaiA [60] makes it improbable that KaiA disassociates into monomeric subunits with that interface exposed [46].

Phosphoryl-S431 of KaiC imposes negative feedback on the KaiA–KaiC interaction

KaiA stimulates KaiC phosphorylation by binding to exposed A-loops [18,61]. Thus, dephosphorylation of KaiC requires sequestration of KaiA away from the A-loops in a KaiA–KaiB–KaiC complex. Interestingly, there seems to be a KaiB-independent negative feedback mechanism on KaiA–KaiC interactions that may facilitate sequestration. The affinity of KaiA for unphosphorylated KaiC is higher than that for phosphorylated KaiC [62,63]. A mathematical model has suggested that such negative feedback could play a role

in maintaining phase coherence across an ensemble of Kai proteins [64]. The high-resolution structure of a complex between KaiA and its binding site on KaiC, which includes the A-loop residues (residues 487–497), suggested that regulation of the A-loops between a KaiA-accessible exposed position and a KaiA-inaccessible buried position (as found in the crystal structure [16]) is a possible mechanism for negative feedback [18]. However, since the A-loops have only been observed in their buried position, the idea of a dynamic equilibrium between buried and exposed positions needed to be tested. As such, A-loop exposure was gauged by the kinetics of their proteolysis, k_{obs} , at a thrombin cut site (LVPRGS) that replaced a naturally occurring stretch of residues, I497–K502, immediately following the A-loop. We reasoned that the accessibility of the proteolysis site would depend on the dynamic equilibrium of the A-loops between buried and exposed positions. We inserted the thrombin cut site in XY-KaiC variants where X and Y, at positions 431 and 432, respectively, were substituted with alanyl/glutamyl residues to mimic the unphosphorylated/phosphorylated states of S431 and T432 of KaiC. Thus, AA-, AE-, EE-, and EA-KaiC variants mimic, respectively, ST-KaiC (unphosphorylated), SpT-KaiC (only T432 phosphorylated), pSpT-KaiC (both residues phosphorylated), and pST-KaiC (only S431 phosphorylated) (Fig. 1b). Several studies have shown that these KaiC mutants are reasonably faithful mimics of the naturally occurring phosphoforms [40,65,66]. Each of the four phosphomimics of KaiC containing the thrombin cut site was incubated with the protease under identical conditions. Time points were analyzed by SDS/PAGE. EA- and EE-KaiC had slower rates of proteolysis, that is, smaller values of k_{obs} , than AA- and AE-KaiC (Fig. 4 and Fig. S6a and b), suggesting that the A-loops made fewer excursions from the buried to the exposed position in the pST- and pSpT-KaiC phosphomimics. Thus, phosphorylation at S431, which tightens the CII ring [23], likely shifts the A-loop equilibrium toward the buried position, where the A-loops can form a ring of hydrogen-bonding interactions that cooperate with phosphoryl-S431 to tighten the CII ring [18].

Because an A-loop comprises one-third of the KaiA binding site [18,20] (the other two-thirds being the C-terminal tail of the CII domain of KaiC), promoting A-loop burial is predicted to weaken KaiA–KaiC binding. Thus, we also measured apparent K_D values, K_D^{app} , of the KaiA–KaiC interaction, as a function of concentration of KaiC phosphomimics, using fluorescence anisotropy of labeled ^{15}N KaiA proteins (Fig. 4 and Fig. S6c). As shown in Fig. 4, the affinity decreases ~10-fold from AE-KaiC to EA-KaiC. Although this change is modest, it should be noted that similarly modest changes were sufficient to reproduce KaiC phosphorylation rhythms *in silico* [63]. In Fig. 4, a trend was observed with smaller k_{obs} correlating with larger K_D^{app} , suggesting that the KaiA-stimulated phosphorylation of S431 imposes negative feedback by promoting burial of part of the KaiA binding site on KaiC. Using just two phosphomimics (AA-KaiC and EE-KaiC), Qin *et al.* reported an opposite trend in KaiA–KaiC affinities using *S. elongatus* proteins [54]. Thus, it was important that we validated our results. Residue E444 of KaiC appears to stabilize the buried form of the A-loops through side-chain hydrogen bonds. Because destabilizing the buried position of the A-loops activates the autokinase activity of KaiC [18], we could gauge the affect of the E444D substitution on the A-loops by its affect on KaiC phosphorylation. In fact, the E444D substitution produced constitutively hyperphosphorylated mutants in both *S. elongatus* [18]

and *T. elongatus* KaiC proteins (Fig. S3c and d). To verify whether E444D indeed acted by destabilizing the A-loops, we measured k_{obs} and K_D^{app} on EA-KaiC containing the E444D substitution. Relative to EA-KaiC, for EA-KaiC^{E444D}, we found a complete reversal of A-loop burial \Leftrightarrow exposure and KaiA–KaiC affinities (Fig. 4). These data suggest that phosphoryl-S431-dependent burial of the A-loops imposes negative feedback regulation on the KaiA–KaiC interaction. This allosteric, KaiB-independent mechanism during the later part of the phosphorylation phase is likely to promote formation of the KaiA–KaiB–KaiC dephosphorylation complex.

KaiA–KaiB–KaiC cooperativity contributes to clock output

In order for circadian clocks to synchronize cellular processes to daily swings in ambient light and temperature, mechanisms must exist to transmit temporal information from the oscillator to other pathways. In cyanobacteria, two mutually antagonistic output pathways, initiated by the SasA and CikA proteins, transduce KaiC phosphorylation rhythms into genome-wide transcription rhythms [47,67]. SasA phosphorylates/activates the transcription factor RpaA, whereas CikA dephosphorylates/deactivates RpaA. SasA is a sensor histidine kinase [42] that, upon binding KaiC, phosphorylates [43] and then transfers the phosphoryl group to the transcription factor RpaA, thereby activating it [44,47,67]. Once activated, RpaA induces transcription of genes such as *kaiBC*. In this way, circadian rhythms of SasA activity drive genome-wide transcription rhythms. SasA binds directly to KaiC using its N-terminal domain [42]. Recently, it was found that KaiB and SasA compete for binding to KaiC [12,46], suggesting that KaiB plays a direct role in regulating clock output [12]. Since the formation of the KaiA–KaiB–KaiC complex is cooperative, we wanted to determine whether KaiA also plays a role in regulating SasA–KaiC interactions. We set up competition experiments between the isolated N-terminal domain of SasA, ^NSasA [68], and KaiB (or KaiB*) \pm KaiA (or \pm ^NKaiA) (Fig. 5 and Fig. S4b and c). In order to minimize KaiA binding to the CII side [18,19], we used a construct of EE-KaiC missing its C-terminal extensions, EE-KaiC⁴⁹⁷ (Fig. 1a) [23]. We also tested ^NSasA and KaiB competition for binding CI*, which was recently identified as their binding site [23,24,45]. Because ^NSasA has no naturally occurring cysteinyl residues, a G57C substitution allowed labeling it with a thiol-reactive fluorophore so that competition could be monitored using fluorescence anisotropy. As seen in Fig. 5 and Fig. S4b and c, the fluorescence anisotropy of free ^NSasA was much lower than when it was bound to EE-KaiC⁴⁹⁷ or CI*, providing sufficient dynamic range for competition experiments. KaiB displaced ^NSasA slowly from EE-KaiC⁴⁹⁷ and CI*. The displacement was significantly faster in the presence of increasing concentration of KaiA [or ^NKaiA (Fig. S4b and c)]. This observation demonstrates that KaiA enhances the competitiveness of KaiB over ^NSasA for KaiC. Therefore, through its role in the cooperativity of KaiA–KaiB–KaiC interactions, KaiA appears to modulate SasA–KaiC interactions, with implications for regulating clock output. Since KaiB* binds KaiC much faster than KaiB [24], it was not surprising that, even in the absence of KaiA, KaiB* quickly displaced ^NSasA (Fig. 5 and Fig. S4b and c).

SasA and KaiB bind to B-loops on CI

To better understand the basis of the competition between SasA and KaiB, we investigated whether they shared binding elements on CI. This identification was aided by sequence alignments between the highly similar [13] RecA-like [14] CI and CII domains of KaiC. As seen in Fig. 6a, CI contains an insertion of several residues (116–123) not found in CII. This insertion is exposed on the bottom of CI as part of a loop, which we named the B-loop (Fig. 1a). The construct, CI* (Fig. 1a), missing the B-loop insertion, retained the structure of CI*, as determined from a comparison of their NMR fingerprints (Fig. S5b). However, unlike with CI*, CI* could not bind ^NSasA or KaiB* (Fig. 6b). This result strongly suggests that the B-loop forms part of the binding site for both proteins. Although the binding sites of ^NSasA and KaiB on CI overlap, their interactions with CI are not identical, as suggested by a comparison of chemical shift perturbations induced by ^NSasA and KaiB* in methyl-TROSY spectra of U-[¹⁵N, ²H]-Ile- δ 1-[¹³C, ¹H]CI* (Fig. 7, rows 1–3).

Perturbations of CI* spectra by KaiB* were not significantly perturbed further by the addition of ^NKaiA, and ^NKaiA by itself did not perturb the spectrum of CI* (Fig. 7, columns 4 and 5), providing further support for the notion that sequestration of KaiA on CI likely does not involve direct KaiA–KaiC interactions but occurs indirectly through KaiA–KaiB interactions. Furthermore, it also suggests that CI adopts the same conformation in the binary KaiB–KaiC and ternary KaiA–KaiB–KaiC complexes. These observations contradict recent studies suggesting that KaiB and SasA bind to the CII side of KaiC [61,69].

Discussion

Based upon our findings, we think that the most stable form of KaiB, the homotetramer [55–57], cannot bind KaiA or KaiC but is in a dynamic equilibrium with transiently disassociated subunits that can bind. Our previous demonstration of slow KaiB–KaiC binding, faster KaiB*–KaiC binding, and subunit shuffling between KaiB proteins supports this notion [24]. Significant changes in NMR spectra of KaiB* after hours of incubation with KaiA (Fig. S5a) also indicate that large changes in the tertiary structure of KaiB occur upon binding, reminiscent of KaiB–KaiC binding [24]. KaiA speeds up KaiB–KaiC binding by shifting KaiB away from the tetramer and toward KaiB subunits active in binding KaiC. In the same way, KaiC enhances the KaiA–KaiB interaction. Thus, formation of the KaiA–KaiB–KaiC dephosphorylation complex on the CI side of KaiC is cooperative. This cooperativity is probably aided by KaiB-independent negative feedback imposed on the KaiA–KaiC interaction on the CII side of KaiC toward the end of the phosphorylation phase. We present our model of the KaiA–KaiB–KaiC interaction in Fig. 8.

Based on EM data, it has been suggested that the competition between SasA and KaiB is on the CII domain of KaiC [61], instead of CI as we propose. The low resolution of the EM data of KaiC makes it difficult to unambiguously distinguish the CI from CII domains, in our opinion. In support of CI binding, another group has independently verified that SasA binds to CI [45]. Additionally, the Rust group showed that the ATPase activity in the CI ring of KaiC was essential for KaiB–KaiC binding [58]. We think that this ATPase activity is dependent on CI-CII ring-stacking interactions, and may be important for exposing the KaiB-binding site [24]. Our identification of the B-loop of CI as a common element of the

KaiB and SasA binding sites adds further support that these interactions take place on CI. Also, NMR spectra of the KaiB*–CI* and ^NSasA–CI* complexes (Fig. 7 and Figs. S5c and S7) argue against artifactual interactions.

Since our data suggest that a single subunit of KaiB binds to a dimer of KaiA, it was important to see how well this stoichiometry agreed with published results, using back-of-the-envelope calculations. It has been shown that KaiB complexation (KaiA–KaiB–KaiC and KaiB–KaiC complexes) lags KaiC phosphorylation by 4–8 h [11,63,70]. When these complexes reach peak levels (at t_{\max} in Fig. S8), ~60% of total KaiB is bound [11]. A new cycle of phosphorylation does not initiate until at least half of these complexes have disassociated (at $t_{1/2}$ in Fig. S8) [11]. Thus, from $t_{\max} \rightarrow t_{1/2}$, KaiA that is desequestered from decomposition of KaiA–KaiB–KaiC complexes would need to be resequenced by intact KaiBC complexes to prevent premature phosphorylation. Using the known dependency of the phosphorylation rhythm on KaiA and KaiB concentrations [71], by our estimation, resequencing is possible when using a stoichiometry of one monomeric subunit of KaiB binding one dimer of KaiA (Table S2 and Fig. S8). In contrast, resequencing of desequestered KaiA from $t_{\max} \rightarrow t_{1/2}$ was not possible when we assumed that a dimer of KaiB sequestered a KaiA dimer [49] or monomer [46]. Thus, the literature lends support to our model. In conclusion, the circadian oscillator of cyanobacteria uses cooperativity to reciprocally regulate periodic formation of complexes on the CI and CII rings of KaiC. This cooperativity likely influences downstream output signaling as well. Thus, understanding the dynamic and allosteric mechanism of the oscillator is an important first step in elucidating how it transduces clock output signals.

Materials and Methods

Protein expression and purification

T. elongatus kaiA, *kaiB*, and *kaiC* genes were cloned into pET-28b by pCr using the NdeI/HindIII sites as described previously [24]. Table S1 presents the abbreviations and complete names of the proteins and corresponding constructs. Proteins were expressed in BL21(DE3) *Escherichia coli* (Novagen) and purified by Ni-NTA affinity chromatography and size-exclusion chromatography as described previously [24], except KaiC proteins were expressed in M9 (H₂O) minimal medium with ¹⁴NH₄Cl for higher purity and yield. Details are provided in Supplementary Material.

Analytical gel-filtration chromatography

All gel-filtration chromatography experiments were performed with a Superdex 200 10/300 GL column (GE Healthcare) as described previously [24], except that the sample injection volume was 250 μ L. Details of experimental setup and proteins used in each experiment are provided in Supplementary Material.

Fluorescence spectroscopy

All data were measured with an ISS PC1 spectrofluorometer. The thiol-reactive fluorophores used for all experiments were 6-iodoacetamidofluorescein (6-IAF) (Invitrogen). The excitation and emission wavelengths were 492 nm and 530 nm, respectively. Data were fit to

a single exponential equation with Mathematica software (Wolfram). Details of experimental setup and proteins used in each experiment are provided in Supplementary Material.

A-loop proteolysis reactions

Each of the five KaiC phosphomimic variants (AA-KaiC, AE-KaiC, EE-KaiC, EA-KaiC, EA-KaiC^{E444D}) with a thrombin cut site (LVPRGS) replacing residues I497–K502 was incubated with thrombin at 30 °C. Aliquots were obtained at indicated time points for SDS/PAGE analysis. Following electrophoresis of 60 V for 30 min and 140 V for 120 min, we stained gels with Coomassie brilliant blue R250 (EMD Chemicals) and determined the percentages of cut product over total protein by densitometry using ImageJ (National Institutes of Health) and PeakFit (SeaSolve Software). k_{obs} values were determined by fitting the thrombin digest kinetics to a single exponential equation using Mathematica software. Details of experimental setup and proteins used in each experiment are provided in Supplementary Material.

In vitro KaiC phosphorylation reactions

Experimental setup was as described previously [24], except that 5 μM KaiC was incubated with 5 μM KaiB and 1.67 μM KaiA or ¹⁵NKaiA at 35 °C. Approximately 100 μL of transparent mineral oil (CMP 25; Cambridge Mill Products, Inc.) was layered on top of the reaction solution to prevent evaporation. Aliquots were obtained at indicated time points for SDS/PAGE analysis. Following electrophoresis as described previously [24], gels were stained with Coomassie brilliant blue R250 (EMD Chemicals), and the percentage of KaiC phosphorylation was determined by densitometry using ImageJ (National Institutes of Health) and PeakFit (SeaSolve Software). Details of experimental setup and proteins used in each experiment are provided in Supplementary Material.

NMR spectroscopy

All NMR experiments were run on a Bruker 600-MHz AVANCE III spectrometer equipped with a TCI cryoprobe. Spectra were processed and analyzed using NMRPipe and NMRDraw [72]. Details of experimental setup and proteins used in each experiment are provided in Supplementary Material.

Supplementary Material

Refer to Web version on PubMed Central for supplementary material.

Acknowledgements

This research was supported by a grant (W911NF-10-1-0090) from the Army. R.T. was supported by a National Science Foundation Graduate Research Fellowship.

Abbreviations used:

EM	electron microscopy
6-IAF	6-iodoacetamidofluorescein

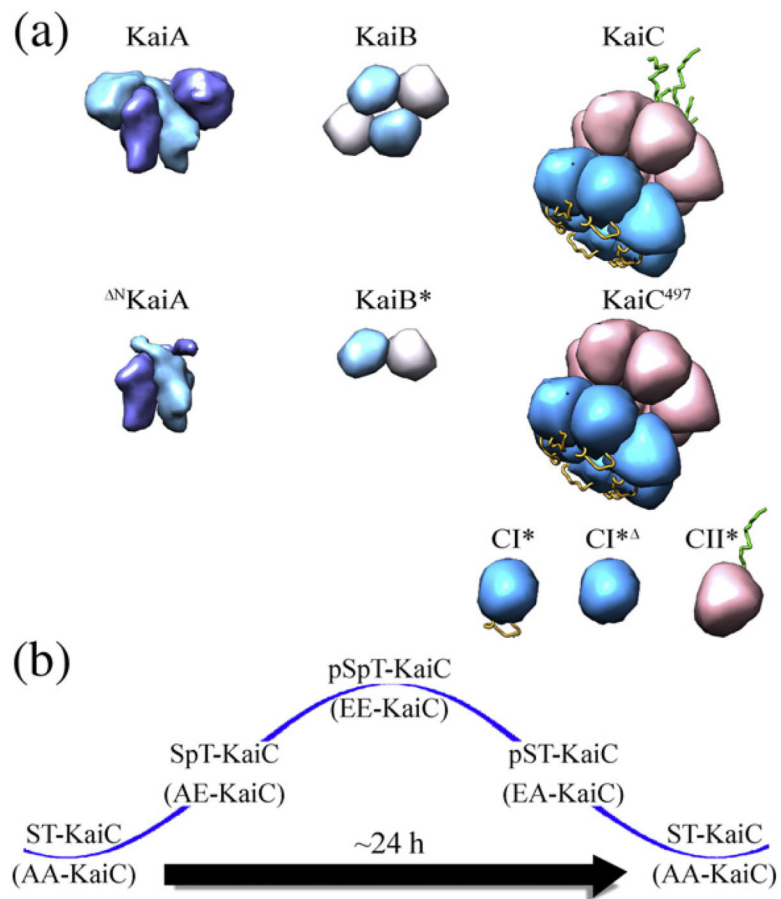
References

- [1]. Dunlap JC, Loros JJ, DeCoursey PJ. Chronobiology: biological timekeeping. Sunderland, MA: Sinauer Associates, Inc.; 2004.
- [2]. Jeyaraj D, Haldar SM, Wan X, McCauley MD, Ripperger JA, Hu K, et al. Circadian rhythms govern cardiac repolarization and arrhythmogenesis. *Nature* 2012;483:96–9. [PubMed: 22367544]
- [3]. Woelfle MA, Ouyang Y, Phanvijhitsiri K, Johnson CH. The adaptive value of circadian clocks: an experimental assessment in cyanobacteria. *Curr Biol* 2004;14:1481–6. [PubMed: 15324665]
- [4]. Oliver P, Sobczyk M, Maywood E, Edwards B, Lee S, Livieratos A, et al. Disrupted circadian rhythms in a mouse model of schizophrenia. *Curr Biol* 2012;22:314–9. [PubMed: 22264613]
- [5]. Goodspeed D, Chehab EW, Min-Venditti A, Braam J, Covington MF. Arabidopsis synchronizes jasmonate-mediated defense with insect circadian behavior. *Proc Natl Acad Sci* 2012;109:4674–7. [PubMed: 22331878]
- [6]. Bass J Circadian topology of metabolism. *Nature* 2012;491:348–56. [PubMed: 23151577]
- [7]. Masri S, Sassone-Corsi P. The circadian clock: a framework linking metabolism, epigenetics and neuronal function. *Nat Rev Neurosci* 2013;14:69–75. [PubMed: 23187814]
- [8]. Ishiura M, Kutsuna S, Aoki S, Iwasaki H, Andersson CR, Tanabe A, et al. Expression of a gene cluster *kaiABC* as a circadian feedback process in cyanobacteria. *Science* 1998;281:1519–23. [PubMed: 9727980]
- [9]. Nakajima M, Imai K, Ito H, Nishiwaki T, Murayama Y, Iwasaki H, et al. Reconstitution of circadian oscillation of cyanobacterial KaiC phosphorylation *in vitro*. *Science* 2005;308:414–5. [PubMed: 15831759]
- [10]. Yoshida T, Murayama Y, Ito H, Kageyama H, Kondo T. Nonparametric entrainment of the *in vitro* circadian phosphorylation rhythm of cyanobacterial KaiC by temperature cycle. *Proc Natl Acad Sci* 2009;106:1648–53. [PubMed: 19164549]
- [11]. Goda K, Ito H, Kondo T, Oyama T. Fluorescence correlation spectroscopy to monitor Kai protein-based circadian oscillations in real time. *J Biol Chem* 2012;287:3241–8. [PubMed: 22157012]
- [12]. Murakami R, Mutoh R, Iwase R, Furukawa Y, Imada K, Onai K, et al. The roles of the dimeric and tetrameric structures of the clock protein KaiB in the generation of circadian oscillations in cyanobacteria. *J Biol Chem* 2012;287:29506–15. [PubMed: 22722936]
- [13]. Iwasaki H, Taniguchi Y, Ishiura M, Kondo T. Physical interactions among circadian clock proteins KaiA, KaiB, and KaiC in cyanobacteria. *EMBO J* 1999;18:1137–45.
- [14]. Leipe DD, Aravind L, Grishin NV, Koonin EV. The bacterial replicative helicase DnaB evolved from a RecA duplication. *Genome Res* 2000;10:5–16. [PubMed: 10645945]
- [15]. Pattanayek R, Mori T, Xu Y, Pattanayek S, Johnson CH, Egli M. Structures of KaiC circadian clock mutant proteins: a new phosphorylation site at T426 and mechanisms of kinase, ATPase and phosphatase. *PLoS One* 2009;4:e7529. [PubMed: 19956664]
- [16]. Pattanayek R, Wang J, Mori T, Xu Y, Johnson CH, Egli M. Visualizing a circadian clock protein: crystal structure of KaiC and functional insights. *Mol Cell* 2004;15:375–88. [PubMed: 15304218]
- [17]. Williams SB, Vakonakis I, Golden SS, LiWang A. Structure and function from the circadian clock protein KaiA of *Synechococcus elongatus*: a potential clock input mechanism. *Proc Natl Acad Sci USA* 2002;99:15357–62. [PubMed: 12438647]
- [18]. Kim Y, Dong G, Carruthers CW, Golden SS, LiWang A. The day/night switch in KaiC, a central oscillator component of the circadian clock of cyanobacteria. *Proc Natl Acad Sci USA* 2008;105:12825–30. [PubMed: 18728181]
- [19]. Pattanayek R, Williams DR, Pattanayek S, Xu Y, Mori T, Johnson CH, et al. Analysis of KaiA–KaiC protein interactions in the cyanobacterial circadian clock using hybrid structural methods. *EMBO J* 2006;25:2017–28. [PubMed: 16628225]
- [20]. Vakonakis I, LiWang A. Structure of the C-terminal domain of the clock protein KaiA in complex with a KaiC-derived peptide: implications for KaiC regulation. *Proc Natl Acad Sci USA* 2004;101:10925–30. [PubMed: 15256595]

- [21]. Rust MJ, Markson JS, Lane WS, Fisher DS, O'Shea EK. Ordered phosphorylation governs oscillation of a three-protein circadian clock. *Science* 2007;318:809–12. [PubMed: 17916691]
- [22]. Nishiwaki T, Satomi Y, Kitayama Y, Terauchi K, Kiyohara R, Takao T, et al. A sequential program of dual phosphorylation of KaiC as a basis for circadian rhythm in cyanobacteria. *EMBO J* 2007;26:4029–37. [PubMed: 17717528]
- [23]. Chang Y, Kuo N, Tseng R, LiWang A. Flexibility of the C-terminal, or CII, ring of KaiC governs the rhythm of the circadian clock of cyanobacteria. *Proc Natl Acad Sci USA* 2011;108:14431–6. [PubMed: 21788479]
- [24]. Chang Y, Tseng R, Kuo N, LiWang A. Rhythmic ring-ring stacking drives the circadian oscillator clockwise. *Proc Natl Acad Sci USA* 2012;109:16847–51. [PubMed: 22967510]
- [25]. Nishiwaki T, Kondo T. The circadian autodephosphorylation of cyanobacterial clock protein KaiC occurs via the formation of ATP as an intermediate. *J Biol Chem* 2012;287:18030–5. [PubMed: 22493509]
- [26]. Egli M, Mori T, Pattanayek R, Xu Y, Qin X, Johnson CH. Dephosphorylation of the core clock protein KaiC in the cyanobacterial KaiABC circadian oscillator proceeds via an ATP synthase mechanism. *Biochemistry* 2012;51:1547–58. [PubMed: 22304631]
- [27]. Kim Y, Vinyard DJ, Ananyev GM, Dismukes GC, Golden SS. Oxidized quinones signal onset of darkness directly to the cyanobacterial circadian oscillator. *Proc Natl Acad Sci* 2012;109:17765–9. [PubMed: 23071342]
- [28]. Ivleva NB, Gao T, LiWang A, Golden SS. Quinone sensing by the circadian input kinase of the cyanobacterial circadian clock. *Proc Natl Acad Sci USA* 2006;103:17468–73. [PubMed: 17088557]
- [29]. Wood TL, Bridwell-Rabb J, Kim Y, Gao T, Chang Y, LiWang A, et al. The KaiA protein of the cyanobacterial circadian oscillator is modulated by a redox-active cofactor. *Proc Natl Acad Sci USA* 2010;107:5804–9. [PubMed: 20231482]
- [30]. Pattanayek R, Sidiqi SK, Egli M. Crystal structure of the redox-active cofactor dibromothymoquinone bound to circadian clock protein KaiA and structural basis for dibromothymoquinone's ability to prevent stimulation of KaiC phosphorylation by KaiA. *Biochemistry* 2012;51:8050–2. [PubMed: 23020633]
- [31]. Schmitz O, Katayama M, Williams SB, Kondo T, Golden SS. CikA, a bacteriophytochrome that resets the cyanobacterial circadian clock. *Science* 2000;289:765–8. [PubMed: 10926536]
- [32]. Mackey SR, Choi J, Kitayama Y, Iwasaki H, Dong G, Golden SS. Proteins found in a CikA interaction assay link the circadian clock, metabolism, and cell division in *Synechococcus elongatus*. *J Bacteriol* 2008;190:3738–46. [PubMed: 18344369]
- [33]. Zhang X, Dong G, Golden SS. The pseudo-receiver domain of CikA regulates the cyanobacterial circadian input pathway. *Mol Microbiol* 2006;60:658–68. [PubMed: 16629668]
- [34]. Gao T, Zhang X, Ivleva NB, Golden SS, LiWang A. NMR structure of the pseudo-receiver domain of CikA. *Protein Sci* 2007;16:465–75. [PubMed: 17322531]
- [35]. Rust MJ, Golden SS, O'Shea EK. Light-driven changes in energy metabolism directly entrain the cyanobacterial circadian oscillator. *Science* 2011;331:220–3. [PubMed: 21233390]
- [36]. Liu Y, Tsinoremas N, Johnson C, Lebedeva N, Golden SS, Ishiura M, et al. Circadian orchestration of gene expression in cyanobacteria. *Genes Dev* 1995;9:1469–78. [PubMed: 7601351]
- [37]. Ito H, Mutsuda M, Murayama Y, Tomita J, Hosokawa N, Terauchi K, et al. Cyanobacterial daily life with Kai-based circadian and diurnal genome-wide transcriptional control in *Synechococcus elongatus*. *Proc Natl Acad Sci* 2009;106:14168–73. [PubMed: 19666549]
- [38]. Vijayan V, Zuzow R, O'Shea EK. Oscillations in supercoiling drive circadian gene expression in cyanobacteria. *Proc Natl Acad Sci USA* 2009;106:22564–8. [PubMed: 20018699]
- [39]. Nakahira Y, Katayama M, Miyashita H, Kutsuna S, Iwasaki H, Oyama T, et al. Global gene repression by KaiC as a master process of prokaryotic circadian system. *Proc Natl Acad Sci USA* 2004;101:881–5. [PubMed: 14709675]
- [40]. Dong G, Yang Q, Wang Q, Kim Y, Wood TL, Osteryoung KW, et al. Elevated ATPase activity of KaiC applies a circadian checkpoint on cell division in *Synechococcus elongatus*. *Cell* 2010;140:529–39. [PubMed: 20178745]

- [41]. Yang Q, Pando BF, Dong G, Golden SS, van Oudenaarden A. Circadian gating of the cell cycle revealed in single cyanobacterial cells. *Science* 2010;327:1522–6. [PubMed: 20299597]
- [42]. Iwasaki H, Williams SB, Kitayama Y, Ishiura M, Golden SS, Kondo T. A KaiC-interacting sensory histidine kinase, SasA, necessary to sustain robust circadian oscillation in cyanobacteria. *Cell* 2000;101:223–33. [PubMed: 10786837]
- [43]. Smith RM, Williams SB. Circadian rhythms in gene transcription imparted by chromosome compaction in the cyanobacterium *Synechococcus elongatus*. *Proc Natl Acad Sci USA* 2006;103:8564–9. [PubMed: 16707582]
- [44]. Takai N, Nakajima M, Oyama T, Kito R, Sugita C, Sugita M, et al. A KaiC-associating SasA-RpaA two-component regulatory system as a major circadian timing mediator in cyanobacteria. *Proc Natl Acad Sci USA* 2006;103:12109–14. [PubMed: 16882723]
- [45]. Valencia SJ, Bitou K, Ishii K, Murakami R, Morishita M, Onai K, et al. Phase-dependent generation and transmission of time information by the KaiABC circadian clock oscillator through SasA-KaiC interaction in cyanobacteria. *Genes Cells* 2012;17:398–419. [PubMed: 22512339]
- [46]. Pattanayek R, Williams DR, Rossi G, Weigand S, Mori T, Johnson CH, et al. Combined SAXS/EM based models of the *S. elongatus* post-translational circadian oscillator and its interactions with the output His-kinase SasA. *PLoS One* 2011;6:e23697. [PubMed: 21887298]
- [47]. Gutu A, O’Shea E. Two antagonistic clock-regulated histidine kinases time the activation of circadian gene expression. *Mol Cell* 2013;50:288–94. [PubMed: 23541768]
- [48]. Iwasaki H, Nishiwaki T, Kitayama Y, Nakajima M, Kondo T. KaiA-stimulated KaiC phosphorylation in circadian timing loops in cyanobacteria. *Proc Natl Acad Sci USA* 2002;99:15788–93. [PubMed: 12391300]
- [49]. Mutoh R, Mino H, Murakami R, Uzumaki T, Takabayashi A, Ishii K, et al. Direct interaction between KaiA and KaiB revealed by a site-directed spin labeling electron spin resonance analysis. *Genes Cells* 2010;15:269–80. [PubMed: 20113360]
- [50]. Golden SS, Ishiura M, Johnson CH, Kondo T. Cyanobacterial circadian rhythms. *Annu Rev Plant Physiol Plant Mol Biol* 1997;48:327–54. [PubMed: 15012266]
- [51]. Garces RG, Wu N, Gillon W, Pai EF. Anabaena circadian clock proteins KaiA and KaiB reveal a potential common binding site to their partner KaiC. *EMBO J* 2004;23:1688–98. [PubMed: 15071498]
- [52]. Uzumaki T, Fujita M, Nakatsu T, Hayashi F, Shibata H, Itoh N, et al. Crystal structure of the C-terminal clock-oscillator domain of the cyanobacterial KaiA protein. *Nat Struct Mol Biol* 2004;11:623–31. [PubMed: 15170179]
- [53]. Sprangers R, Kay LE. Quantitative dynamics and binding studies of the 20S proteasome by NMR. *Nature* 2007;445:618–22. [PubMed: 17237764]
- [54]. Qin X, Byrne M, Mori T, Zou P, Williams DR, Mchaourab H, et al. Intermolecular associations determine the dynamics of the circadian KaiABC oscillator. *Proc Natl Acad Sci USA* 2010;107:14805–10. [PubMed: 20679240]
- [55]. Pattanayek R, Williams DR, Pattanayek S, Mori T, Johnson CH, Stewart PL, et al. Structural model of the circadian clock KaiB–KaiC complex and mechanism for modulation of KaiC phosphorylation. *EMBO J* 2008;27:1767–78. [PubMed: 18497745]
- [56]. Hitomi K, Oyama T, Han S, Arvai AS, Getzoff ED. Tetrameric architecture of the circadian clock protein KaiB: a novel interface for intermolecular interactions and its impact on the circadian rhythm. *J Biol Chem* 2005;280:19127–35. [PubMed: 15716274]
- [57]. Iwase R, Imada K, Hayashi F, Uzumaki T, Morishita M, Onai K, et al. Functionally important substructures of circadian clock protein KaiB in a unique tetramer complex. *J Biol Chem* 2005;280:43141–9. [PubMed: 16227211]
- [58]. Phong C, Markson JS, Wilhoite CM, Rust MJ. Robust and tunable circadian rhythms from differentially sensitive catalytic domains. *Proc Natl Acad Sci* 2013;110:1124–9. [PubMed: 23277568]
- [59]. Ye S, Vakonakis I, Ioerger TR, LiWang A, Sacchettini JC. Crystal structure of circadian clock protein KaiA from *Synechococcus elongatus*. *J Biol Chem* 2004;279:20511–8. [PubMed: 15007067]

- [60]. Vakonakis I, Sun J, Wu T, Holzenburg A, Golden SS, LiWang A. NMR structure of the KaiC-interacting C-terminal domain of KaiA, a circadian clock protein: implications for the KaiA–KaiC interaction. *Proc Natl Acad Sci USA* 2004;101: 1479–84. [PubMed: 14749515]
- [61]. Pattanayek R, Yadagiri KK, Ohi MD, Egli M. Nature of KaiB–KaiC binding in the cyanobacterial circadian oscillator. *Cell Cycle* 2013;12:810–7. [PubMed: 23388462]
- [62]. Hayashi F, Ito H, Fujita M, Iwase R, Uzumaki T, Ishiura M. Stoichiometric interactions between cyanobacterial clock proteins KaiA and KaiC. *Biochem Biophys Res Commun* 2004;316:195–202. [PubMed: 15003530]
- [63]. Ma L, Ranganathan R. Quantifying the rhythm of KaiB–C interaction for in vitro cyanobacterial circadian clock. *PLoS One* 2012;7:e42581. [PubMed: 22900029]
- [64]. van Zon JS, Lubensky DK, Altena PRH, ten Wolde PR. An allosteric model of circadian KaiC phosphorylation. *Proc Natl Acad Sci USA* 2007;104:7420–5. [PubMed: 17460047]
- [65]. Murayama Y, Mukaiyama A, Imai K, Onoue Y, Tsunoda A, Nohara A, et al. Tracking and visualizing the circadian ticking of the cyanobacterial clock protein KaiC in solution. *EMBO J* 2011;30:68–78. [PubMed: 21113137]
- [66]. Terauchi K, Kitayama Y, Nishiwaki T, Miwa K, Murayama Y, Oyama T, et al. ATPase activity of KaiC determines the basic timing for circadian clock of cyanobacteria. *Proc Natl Acad Sci USA* 2007;104:16377–81. [PubMed: 17901204]
- [67]. Taniguchi Y, Takai N, Katayama M, Kondo T, Oyama T. Three major output pathways from the KaiABC-based oscillator cooperate to generate robust circadian kaiBC expression in cyanobacteria. *Proc Natl Acad Sci USA* 2010;107:3263–8. [PubMed: 20133618]
- [68]. Vakonakis I, Klewer DA, Williams SB, Golden SS, LiWang AC. Structure of the N-terminal domain of the circadian clock-associated histidine kinase SasA. *J Mol Biol* 2004;342:9–17. [PubMed: 15313603]
- [69]. Villarreal SA, Pattanayek R, Williams DR, Mori T, Qin X, Johnson CH, et al. CryoEM and molecular dynamics of the circadian KaiB–KaiC complex indicates that KaiB monomers interact with KaiC and block ATP binding clefts. *J Mol Biol* 2013;425:3311–24. [PubMed: 23796516]
- [70]. Kageyama H, Nishiwaki T, Nakajima M, Iwasaki H, Oyama T, Kondo T. Cyanobacterial circadian pacemaker: Kai protein complex dynamics in the KaiC phosphorylation cycle *in vitro*. *Mol Cell* 2006;23:161–71. [PubMed: 16857583]
- [71]. Nakajima M, Ito H, Kondo T. *In vitro* regulation of circadian phosphorylation rhythm of cyanobacterial clock protein KaiC by KaiA and KaiB. *FEBS Lett* 2010;584:898–902. [PubMed: 20079736]
- [72]. Delaglio F, Grzesiek S, Vuister GW, Zhu G, Pfeifer J, Bax A. NMRPipe: a multidimensional spectral processing system based on UNIX pipes. *J Biomol NMR* 1995;6:277–93. [PubMed: 8520220]

**Fig. 1.**

A summary of KaiABC oscillator proteins and their variants used in this study. (a) Pictorial representations of wild-type cyanobacterial clock proteins: KaiA, KaiB, and KaiC as, respectively, homodimer, homotetramer, and homohexamer. Important variants of KaiA and KaiB and KaiC proteins used in this study are shown as well: ^{ΔN}KaiA (missing its N-terminal domain by truncating before residue S147), KaiB* (a dimeric variant by truncating after residue Y94 and with Y8A and Y94A substitutions) [24], KaiC⁴⁹⁷ (missing A-loops by truncating after I497) [18], CI* (monomeric CI domain: KaiC residues 1–247, with R41A and K173A substitutions) [24], CI*^Δ (same as CI*, but with the deletion of B-loop from residues 116–123), and CII* (monomeric CII domain: KaiC residues 249–518, with S431E, T432E, and E444D substitutions). Complete construct information is provided in Table S1. (b) A phosphorylation cycle of KaiC. ST-KaiC (unphosphorylated), SpT-KaiC (T432 phosphorylated), pSpT-KaiC (S431 and T432 phosphorylated), and pST-KaiC (S431 phosphorylated) can be mimicked by, respectively, AA-KaiC, AE-KaiC, EE-KaiC, and EA-KaiC. Alanine/glutamine substitutions mimic the unphosphorylated/phosphorylated states of S431 and T432.

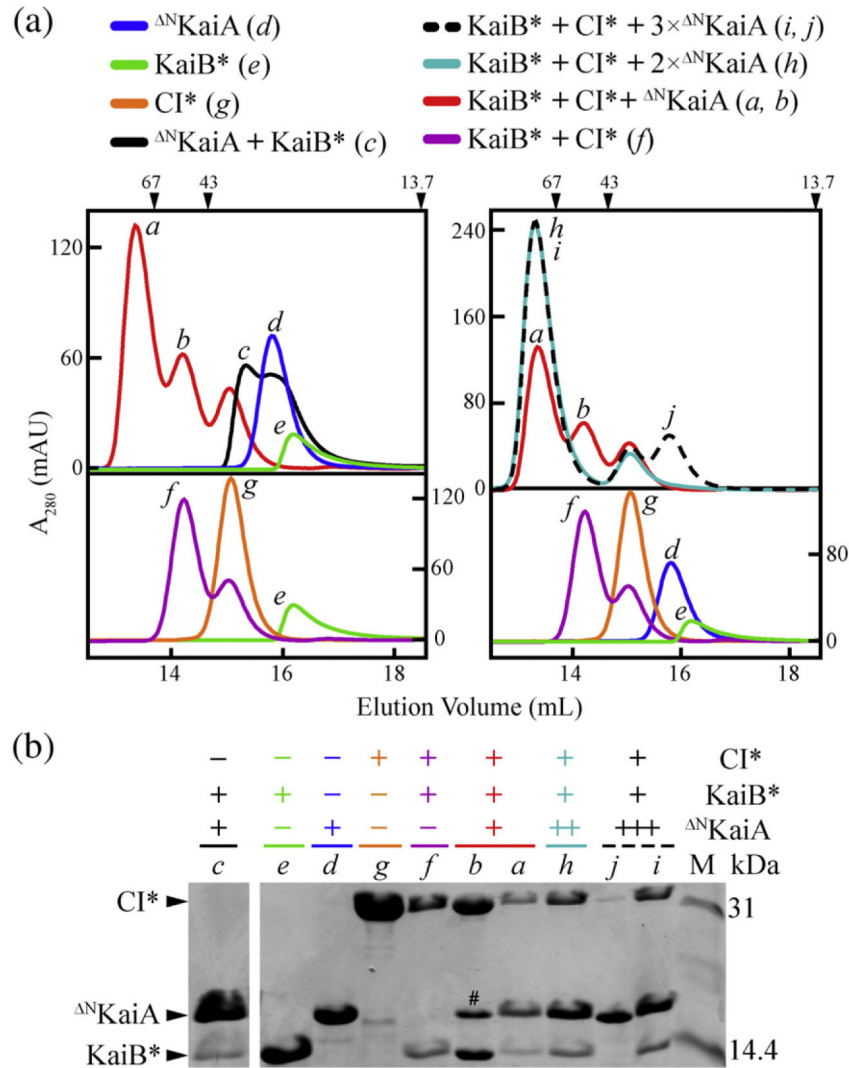


Fig. 2. Formation of Δ^N KaiA–KaiB*–CI* and Δ^N KaiA–KaiB* complexes. (a) Gel-filtration profiles of KaiB* + CI* + Δ^N KaiA (red), Δ^N KaiA + KaiB* (black), Δ^N KaiA alone (blue), and KaiB* alone (green) (top left). Control mixtures of KaiB* + CI* (purple), CI* alone (orange), and KaiB* alone (green) are shown below for comparison (bottom left). Gel-filtration profiles of KaiB* + CI* + Δ^N KaiA with increasing amounts of Δ^N KaiA added are shown on the top right panel (1 \times , red; 2 \times , cyan; 3 \times , black dash). Control mixtures of KaiB* + CI* (purple), CI* alone (orange), Δ^N KaiA alone (blue), and KaiB* alone (green) are shown below for comparison (bottom right). 1 \times corresponds to 50 μ M monomer concentration. Chromatogram of Δ^N KaiA + CI* is shown in Fig. S1a. Molecular mass markers in kilodaltons (kDa) are marked by black arrows along the top of the gel-filtration chromatograms. Peaks denoted by *a*, *b*, *c*, *d*, *e*, *f*, *g*, *h*, *i*, and *j* were checked by SDS/PAGE. For details on the protein constructs and experimental setup, please see Table S1. (b) SDS/PAGE gel of peaks *a*, *b*, *c*, *d*, *e*, *f*, *g*, *h*, *i*, and *j* in (a). All lanes shown were run on the same gel. The band marked “#” in lane *b* indicates the presence of Δ^N KaiA in peak *b*. A comparison of peak *b* with peaks from other chromatograms (*f*, *h*, and *i*) suggests that the

presence of $^{15}\text{N}\text{KaiA}$ in b was likely due to overlap of peaks a and b in the 1:1:1 $^{15}\text{N}\text{KaiA}:\text{KaiB}^*:\text{CI}^*$ chromatogram. The presence of a peak corresponding to free CI^* in the 1:1:1, 2:1:1, and 3:1:1 $^{15}\text{N}\text{KaiA}:\text{KaiB}^*:\text{CI}^*$ chromatograms suggests that the true concentration of CI^* was systematically underestimated. This underestimation however did not affect our analysis because CI^* and $^{15}\text{N}\text{KaiA}$ do not interact with each other directly.

Author Manuscript

Author Manuscript

Author Manuscript

Author Manuscript

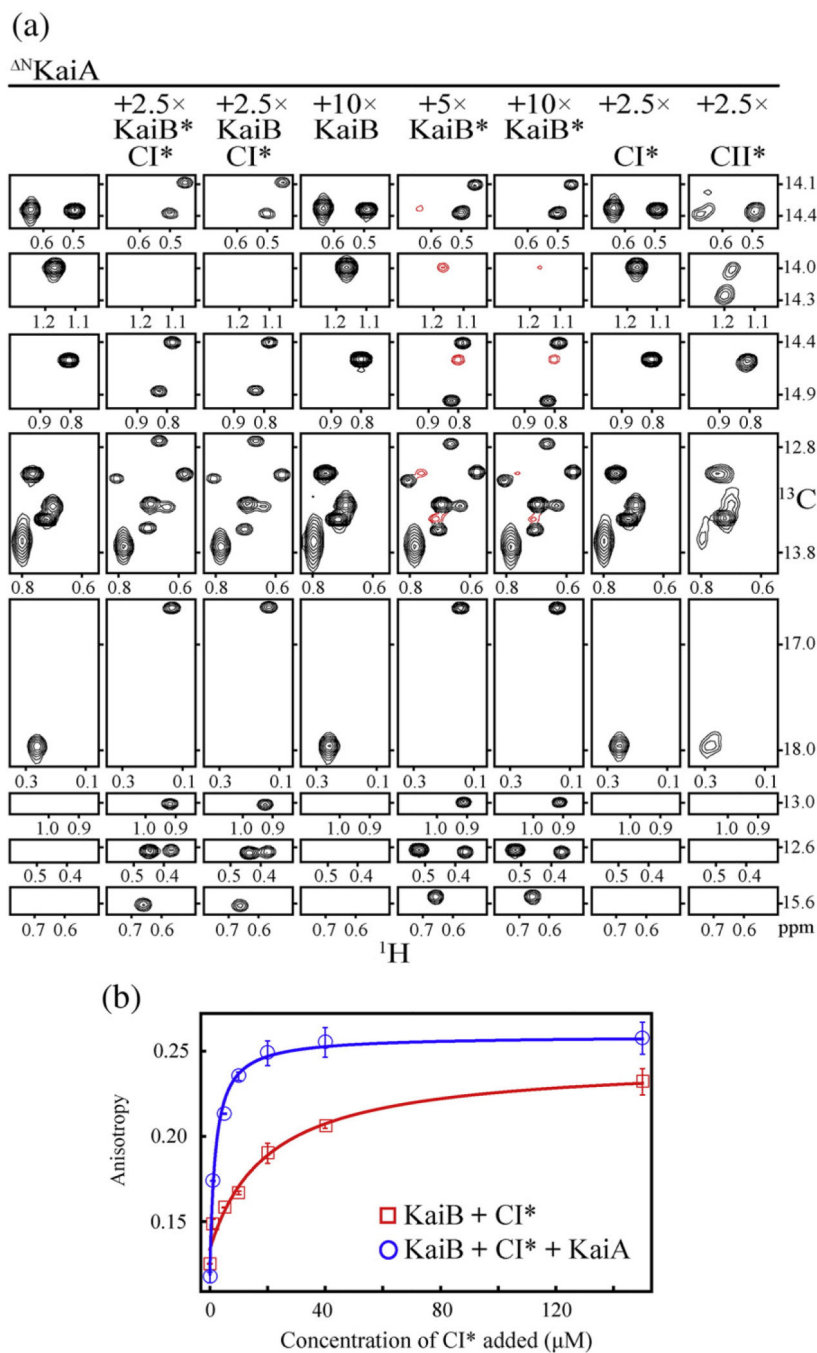


Fig. 3. Formation of a ^{15}N KaiA–KaiB*–CI* complex is a cooperative process. (a) Selected regions from methyl-TROSY spectra of $1 \times U$ - $[^{15}\text{N}, ^2\text{H}]$ -Ile δ 1- $[^{13}\text{C}, ^1\text{H}]$ ^{15}N KaiA alone (column 1) or in the presence of $2.5\times$ (KaiB* + CI*) (column 2), $2.5\times$ (KaiB + CI*) (column 3), $10\times$ KaiB (column 4), $5\times$ KaiB* (column 5), $10\times$ KaiB* (column 6), $2.5\times$ CI* (column 7), or $2.5\times$ CII* (column 8). $1 \times$ corresponds to $20 \mu\text{M}$ monomer concentration. NMR peaks marked in red are at positions that correspond to resonances in free ^{15}N KaiA (columns 4 and 5). Full spectra are shown in Fig. S2. For details on the protein constructs and experimental

setup, please see Table S1.(b) Fluorescence anisotropy data to measure apparent dissociation constants, K_D^{app} , of 6-IAF-labeled KaiB binding to CI* in the presence (blue) or absence (red) of 5 μM KaiA. Data were fit to equation (2) in Supplementary Material. The K_D^{app} values for CI* and CI* + KaiA are 20.5 ± 1.0 and $2.0 \pm 0.4 \mu\text{M}$, respectively. Standard error was estimated from duplicate measurements. Equilibrium prior to measurements was achieved by incubation of samples for 24 h (Fig. S4a). For details on the protein constructs and experimental setup, please see Table S1.

Author Manuscript

Author Manuscript

Author Manuscript

Author Manuscript

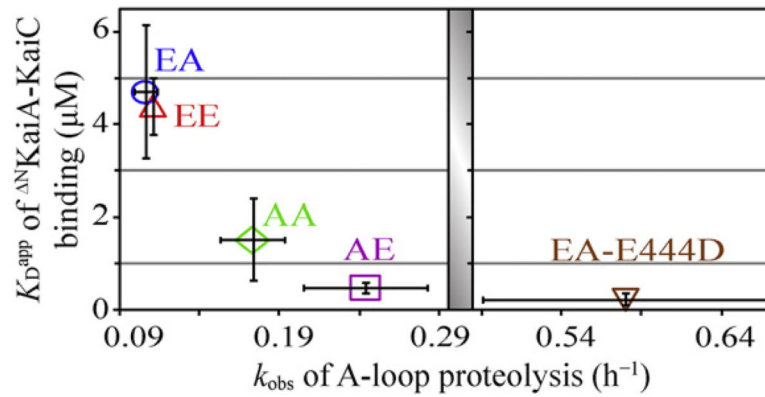


Fig. 4.

A-loop exposure is correlated with KaiA–KaiC affinity. Kinetics of A-loop proteolysis of five variants of KaiC (AA-KaiC, green diamond; AE-KaiC, purple square; EE-KaiC, red triangle; EA-KaiC, blue circle; EA-KaiC^{E444D}, brown inverted triangle) with a thrombin cut site (LVPRGS) replacing residues I497 to K502. A-loop proteolysis rates were determined by fitting time points resolved by SDS/PAGE (Fig. S6a and b) to equation (5) in Supplementary Material. k_{obs} (h^{-1}) for Aa-, AE-, EE-, EA-, and EA-E444D are 0.17 ± 0.02 , 0.24 ± 0.04 , 0.111 ± 0.001 , 0.106 ± 0.007 , and 0.58 ± 0.09 , respectively. ^{15}N KaiA–KaiC affinity, $K_{\text{D}}^{\text{app}}$, was determined from the dependence of fluorescence anisotropy of 6-IAF labeled ^{15}N KaiA on the concentration of the same five phosphomimic variants of KaiC, but without the thrombin cut sites. The $K_{\text{D}}^{\text{app}}$ values, obtained from fitting the data to equation (1) in the Supplementary Material, for AA-, AE-, EE-, EA-, and EA-E444D are 1.5 ± 0.9 , 0.5 ± 0.1 , 4.4 ± 0.6 , 4.7 ± 1.4 , and 0.2 ± 0.1 μM , respectively (Fig. S6c). Standard errors for k_{obs} and $K_{\text{D}}^{\text{app}}$ were estimated from duplicate measurements as shown in Fig. S6. For details on the protein constructs and experimental setup, please see Table S1.

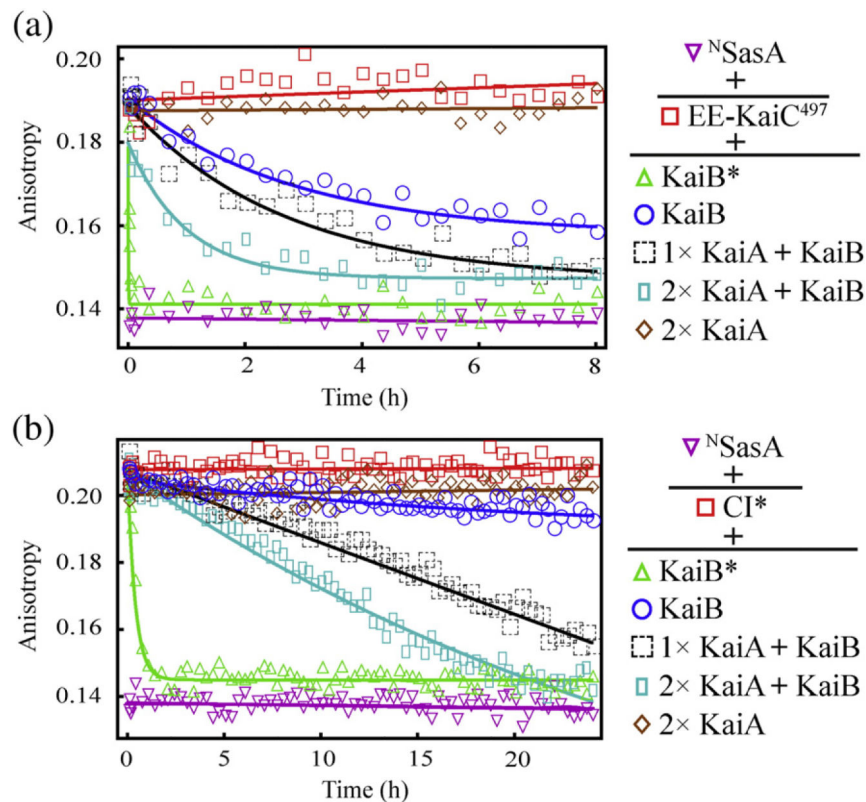


Fig. 5.

KaiA as a modulator of KaiB/SasA competition for KaiC and CI. (a) Fluorescence anisotropy of competition kinetics of 6-IAF-labeled N SasA alone (purple), N SasA + EE-KaiC⁴⁹⁷ (red), N SasA + EE-KaiC⁴⁹⁷ + KaiB* (green), N SasA + EE-KaiC⁴⁹⁷ + KaiB (blue), N SasA + EE-KaiC⁴⁹⁷ + KaiB + 1 × KaiA (black), N SasA + EE-KaiC⁴⁹⁷ + KaiB + 2 × KaiA (cyan), and N SasA + EE-KaiC⁴⁹⁷ + 2 × KaiA (brown). 1 × corresponds to 10 μM monomer concentration. For details on the protein constructs and experimental setup, please see Table S1. Details on fitting the data to a single exponential equation are provided in the Supplementary Material. (b) Fluorescence anisotropy of competition kinetics of 6-IAF-labeled N SasA alone (purple), N SasA + CI* (red), N SasA + CI* + KaiB* (green), N SasA + CI* + KaiB (blue), N SasA + CI* + KaiB + 1 × KaiA (black), N SasA + CI* + KaiB + 2 × KaiA (cyan), and N SasA + CI* + 2 × KaiA (brown). 1 × corresponds to 10 μM monomer concentration. For details on the protein constructs and experimental setup, please see Table S1. Differences in the kinetics between (a) and (b) suggest that the hexameric EE-KaiC⁴⁹⁷ and monomeric CI* do not interact identically with N SasA and KaiB.

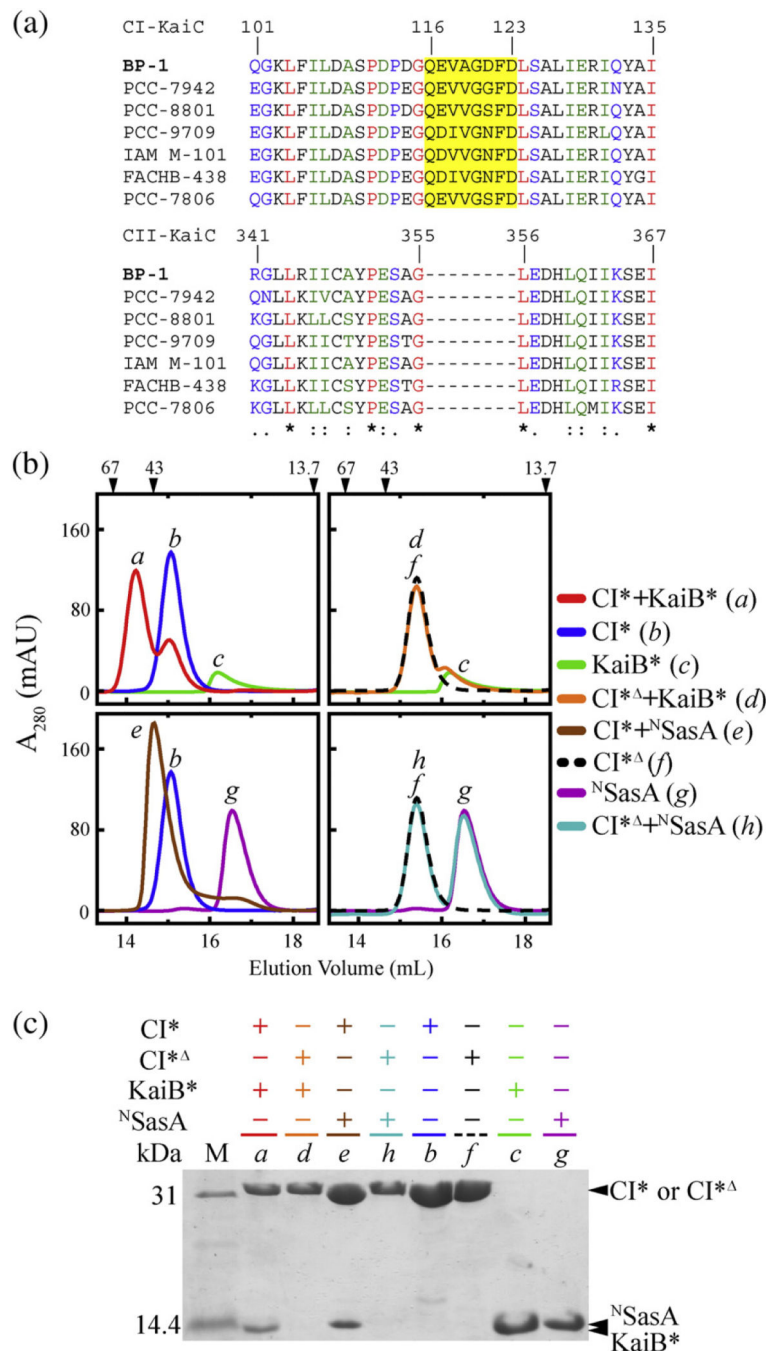


Fig. 6. ^NSasA and KaiB* compete on CI near the B-loops. (a) CLUSTAL-W multiple sequence alignment of the two domains of KaiC from different cyanobacteria species reveals an insertion in CI missing in CII. The insertion, termed the “B-loop”, is from residues 116 to 123 (highlighted in yellow). Sequences correspond to the following strains: BP-1, *T. elongatus* BP-1 (used in this study); PCC-7942, *S. elongatus* PCC-7942; PCC-8801, *Synechococcus* sp. PCC-8801; PCC-9709, *Nostoc* sp. PCC-9709; IAM M-101, *Lentinula boryana* IAM M-101; FACHB-438, *Acanthastrea maxima* FACHB-438; PCC-7806, *Microcystis*

aeruginosa PCC-7806.(b) Gel-filtration profiles of CI* + KaiB* (red, from Fig. 1a), CI* + ^NSasA (brown), CI* + KaiB* (orange), and CI* + ^NSasA (cyan). CI* is with B-loop (residues 116–123) deleted. Peaks denoted by a, b, c, d, e, f, g, and h were checked by SDS/PAGE. Molecular mass markers in kilodaltons are marked by black arrows along the top of the gel-filtration chromatograms. For details on the protein constructs and experimental setup, please see Table S1.(c) SDS/PAGE gel of peaks a, b, c, d, e, f, g, and h in (b).

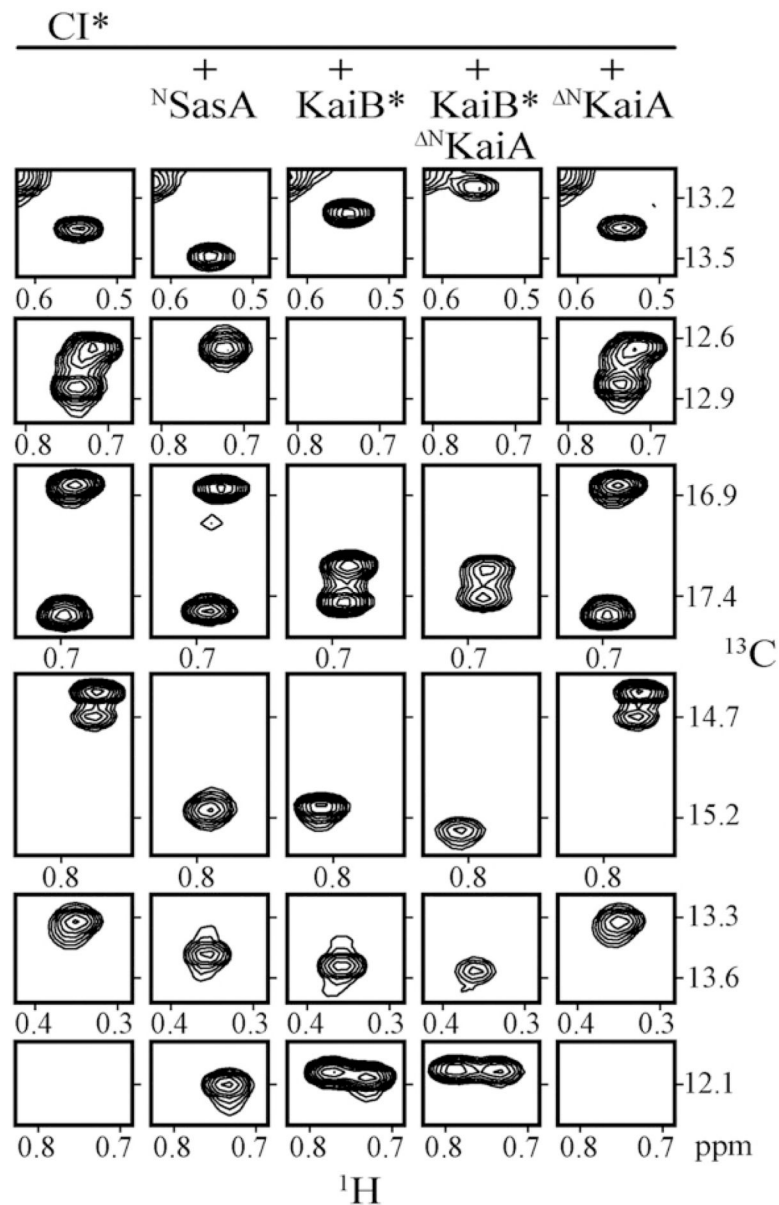


Fig. 7. ^NSasA and KaiB* do not interact identically with CI. Selected regions from methyl-TROSY spectra of U-[¹⁵N, ²H]-Ileδ1-[¹³C, ¹H]-labeled CI* alone (column 1), in the presence of ^NSasA (column 2), KaiB* (column 3), KaiB* + ^NKaiA (column 4), or ^NKaiA (column 5). Full spectra are shown in Fig. S7. For details on the protein constructs, please see Table S1.

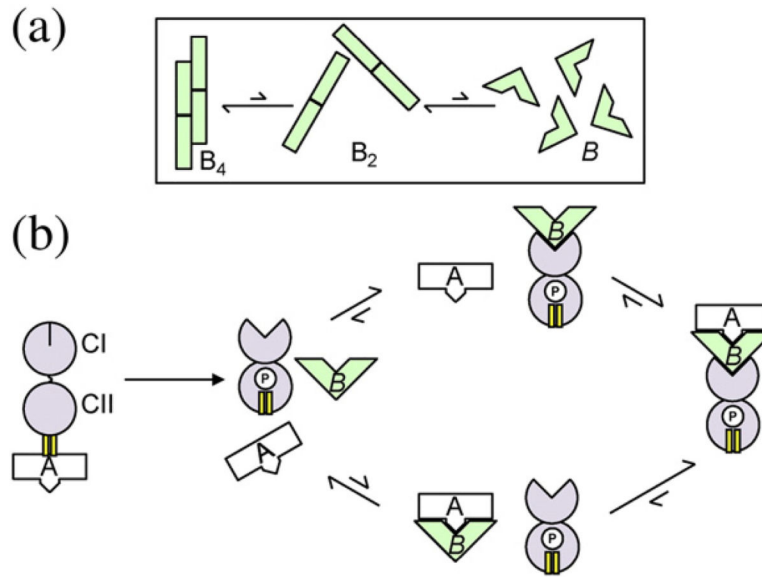


Fig. 8. Model of cooperative formation of the KaiABC dephosphorylation complex. (a) KaiB exists in a dynamic equilibrium between distinct quaternary states: tetramer (B_4), dimer (B_2), and active monomer (B). B_4 is the most stable form [55–57], whereas B is a highly transient state. (b) The CI domain of KaiC and KaiA can each stabilize the highly active monomer of KaiB, B , thereby cooperatively forming the KaiABC dephosphorylation complex. A-loops of KaiC are depicted as yellow bars. P indicates phosphorylation at S431 of KaiC. Upon S431 phosphorylation, two major allosteric events occur in KaiC: (1) The A-loops are shifted toward their buried position due to CII-ring tightening [23], and KaiA consequently loses affinity for the CII domain. (2) The CI and CII domains of KaiC stack together, exposing the KaiB binding site on CI [24]. Now, the CI domain can selectively capture the highly transient B , enhancing KaiA sequestration. Alternatively, KaiA can selectively capture B , thereby promoting binding to KaiC.